PHYSICAL REVIEW D VOLUME 21, NUMBER 7 1 APRIL 1980

Baryon decays in a quark model with chromodynamics

Roman Koniuk and Nathan Isgur
Department of Physics, University of Toronto, Toronto, Canada M5S 1A7
(Received 6 December 1979)

Quark models of hadrons are tested in a very limited way when only their spectroscopy is compared with experiment; at least equally important tests arise from examining the predicted internal structure of the hadrons via analysis of their decay amplitudes. We present here a compilation of one of the most extensive calculations of baryon amplitudes to date, encompassing the pseudoscalar and photon couplings of the states associated with up to two orbital or one radial excitation in the nonrelativistic quark model. These amplitudes are then combined with the baryon compositions predicted by a quark model incorporating some of the features expected to arise from quantum chromodynamics. The result is to generate a set of baryon amplitudes which (1) resolve the problem of "missing" resonances by essentially decoupling a very large number of states from partial-wave analyses and (2) leave those resonances which remain in remarkable correspondence to the observed states in both their masses and decay amplitudes.

I. INTRODUCTION

A successful model of hadron structure must explain many things at once. The most obvious features of a given hadron are its mass, spin, flavor, and parity quantum numbers and these must certainly be given by the model for all hadrons. These properties alone, however, are not very conclusive: The prediction of spin and parities may simply reflect some underlying symmetry of the model, while a given (approximate) mass spectrum for a limited number of states may arise from several different patterns of forces. Much more definitive in some ways are hadronic properties which are not simply quantum numbers, so that they mirror the internal structure of the states. Various low-energy properties such as magnetic moments, charge radii, etc., are of this type, but the most useful and extensive of such properties are decay amplitudes: A hadronic model which predicts with precision the mass, spin, and parity of a state can be eliminated if it improperly predicts its decay widths. These various widths, which usually involve the matrix elements of constituent operators, are testing rather directly the model's predictions for the internal structure of the hadron in question.

In this paper we discuss the results of an extensive analysis of baryon couplings based on simple models of pseudoscalar-meson and photon emission and a quark model for baryon structure with features suggested by chromodynamics. The primary goal of the work we are describing here is to test the model for baryon structure. As a consequence, our approach was very different from that employed in most previous baryon-decay analyses which have been concerned mainly with testing models for the decay processes themselves. The strategy employed in such analyses was to parametrize the baryon structure in a very general way and then perform a fit to decay amplitudes subject to variation of these parameters. In many instances this method was very successful, so that one could actually deduce from the decay amplitudes an approximate description of the structure of certain of the decaying baryons. Since to a large degree this strategy tends to "decouple" the decay and baryon-structure models, it is very desirable. Unfortunately, once the parametrization of baryon structure becomes very complex, the method breaks down. For example, certain sectors of the positive-parity baryons, which we will discuss below, would require 28 mixing angles for their parametrization while the available data correspond to only a few measured decay amplitudes. Given our aims and these difficulties, we followed the obvious route: We have coupled the predicted baryon structure of the model we are studying with a decay model (about which we maintain a healthy skepticism) to directly predict decay amplitudes. This allows us to compare with essentially every piece of experimental information, even in complicated sectors such as the one mentioned above.

The amplitudes predicted in this way have the property that (1) they essentially decouple a very large number of resonances from partial-wave analyses thereby resolving the problem of "missing" states, and (2) they leave the states which remain in remarkable correspondence to the observed states in both their masses and in the sign and magnitude of their decay amplitudes. This indicates to us that both the decay model and the model for baryon structure are essentially correct, at least in the sense that they provide a good overall—even if by no means precise—des-

cription of baryonic properties. In the next two sections we will describe these models. In Sec. II we will give a very brief review of the quark model with chromodynamics which has been extensively applied to the study of baryons. In Sec. III we will discuss our models for pseudoscalar meson and photon emission which are essentially slightly reinterpreted versions of the standard nonrelativistic models for these processes. In the same section we discuss our calculations of the decay amplitudes and present tabulations which include decay amplitudes for all the states associated with the low-lying SU(6) multiplets $(56,0^+)$, $(70,1^-)$, $(56',0^+)$, $(70,0^+)$, $(56,2^+)$, $(70,2^+)$, and $(20,1^+)$, i.e., states with up to two units of orbital angular momentum or up to one unit of radial excitation in the nonrelativistic quark model. We believe that this is one of the most extensive tabulations of this type to date. Drawing on the structure predicted for the baryons by the model of Sec. II, we then present in Sec. IV the comparison between the predicted and measured decay amplitudes for all $S=0$ and -1 baryons associated with the above-mentioned multiplets. Section V contains various comments and our conclusions.

II. A QUARK MODEL FOR BARYONS WITH CHROMODYNAMICS

The model[1-7] for baryon structure which is the basis of this analysis has been fully described in several places[8-11]; we shall restrict ourselves here to a brief review. The model begins with the foundations[12,13] laid by Dalitz, Greenberg, and their collaborators, who originated the nonrelativistic three-quark model of the baryons, and builds upon it a structure based on ideas suggested by—but not derived from—quantum chromodynamics[14-16] (QCD). The three main new ingredients of the model are the following:

(1) Quark confinement. It is assumed, based on the color-flux-tube model, that quarks i and j are subject to a long-range two-body potential

$$V_{qq}(r_{ij}) = -V(r_{ij})\tfrac{1}{2}\vec{\lambda}_i \cdot \tfrac{1}{2}\vec{\lambda}_j , \tag{1}$$

where $V(r_{ij})$ is a confining potential which is flavor and spin independent and the λ's are the Gell-Mann SU(3) matrices.[17]

(2) One-gluon exchange. With the long-range nonperturbative confinement presumed to be described by V_{qq}, it is next assumed that the remainder of the interquark interaction at short distances can be adequately approximated by one-gluon exchange.

(3) Approximately pointlike constituent quarks. With the nonliberation of quarks ensured by the confinement potential, it is assumed that quark masses have their pointlike values, i.e., the values associated with the Dirac moments that are required to explain the magnetic moments of the baryons.

In practice, several approximations are made to extract predictions from the model just sketched. First, the full spin-independent interaction between quarks (including the confinement, Coulomb, orbit-orbit, etc., interactions) is written in the form

$$\tfrac{1}{2}Kr_{ij}^2 + U(r_{ij}) \tag{2}$$

and $U(r_{ij})$ is treated as a perturbation. There are two approximations here, that U is small, and that k and U remain approximately flavor independent. Consistent with the approximation that U is small, the hyperfine interaction

$$H_{\rm hyp}=\sum_{i<j}\frac{2\alpha_s}{3m_i m_j}\left[\frac{8\pi}{3}\vec{S}_i\cdot\vec{S}_j\delta^3(\vec{r}_{ij}) + \frac{1}{r_{ij}^3}\left(\frac{3\vec{S}_i\cdot\vec{r}_{ij}\vec{S}_j\cdot\vec{r}_{ij}}{r_{ij}^2}-\vec{S}_i\cdot\vec{S}_j\right)\right] \tag{3}$$

is then treated perturbatively in harmonic-oscillator wave functions. Here, in addition to assuming that α_s and m_i are not q^2 dependent, only nearest-neighbor (corresponding to states at $\pm 2\omega$ in the harmonic-oscillator model) mixing is taken into account. Finally, because of the effects of Thomas precession, in the actual calculations spin-orbit effects are treated rather empirically. Since they turn out to be small, in the end the physics of the model may be summarized as consisting simply of flavor-independent "confinement" perturbed by hyperfine interactions.

In spite of these approximations—not to mention the nonrelativistic approximation and the oversimplified model with which we begin—one can hope that if the dynamics of the model is basically correct, the resulting picture of the baryons will reflect the dominant features observed in nature. We shall see in what follows that this seems to be the case.

III. THE DECAY AMPLITUDES

Since it is our purpose to study decays of baryons from the quark model reviewed in Sec. II, it is natural and consistent to describe the decay amplitudes in the explicit nonrelativistic quark-model approach.[18-20] We find, in any event, that the alternatives—namely, the group-theoretical schemes such as l-broken $SU(6)_W$ (Ref. 21) or relativistic quark models[22]—are, once their parameters have been chosen, very similar in

their predictions.

In our variation on the classical nonrelativistic quark-model approach, the decay of a baryon is assumed to proceed through a single quark transition as depicted in Figs. 1(a) for photonic and 1(b) for mesonic transitions.

The amplitude for photodecay in the model is obtained by making a nonrelativistic reduction of the pointlike γ^μ quark-photon interaction; upon sandwiching this interaction between initial and final states for the process $B \to B'\gamma$ one obtains the T-matrix element

$$\langle B'(p's')\gamma(K\lambda)|T|B(ps)\rangle = -\frac{3ie}{(2\pi)^{3/2}}\left\langle B'(p's')\left|\frac{e_3}{e}\left[\frac{\vec{\sigma}_3\cdot(\vec{K}\times\epsilon^*)}{2m}+i\frac{\vec{p}_3'\cdot\vec{\epsilon}^*}{m}\right]e^{-i\vec{K}\cdot\vec{r}_3}\right|B(ps)\right\rangle, \tag{4}$$

where $\vec{\epsilon}(K\lambda)$ is the photon polarization vector, e_3, $\frac{1}{2}\vec{\sigma}_3$, and $\vec{r}_3$ are the charge, spin, and position of the third quark, and $\vec{p}_3'$ is the momentum of the third quark in B' (we have used overall permutation symmetry to set the full decay amplitude to three times the amplitude for emission from the third quark). Since we consider here only the case where B' is a nucleon, one obtains at most two independent helicity amplitudes. Apart from an overall normalization, the result (4) is that of Copley, Karl, and Obryk[19] (see subsection 5 of the Appendix for details of our amplitude conventions).

The amplitude for pseudoscalar meson emission is less well-founded. In the simplest case, meson emission can occur by the creation of a single quark-antiquark pair via the diagrams of Fig. 2. Analysis of meson decay processes indicates that the creation of $u\bar{u}$, $d\bar{d}$, and $s\bar{s}$ pairs is SU(3) symmetric to a good approximation, and we shall assume here that this is the case. In this event the diagram of Fig. 2(b) contributes only to the creation of the SU(3)- singlet meson $\eta_1 \equiv (1/\sqrt{3})(u\bar{u}+d\bar{d}+s\bar{s})$ and since the η-η' mixing angle is only about -10^0, this diagram will have little effect on our predictions for the η (we do not consider η' decays). There are two reasons why the effects of Fig. 2(b) may be additionally suppressed: (1) They are Okubo-Zweig-Iizuka-rule-violating, and (2) at least part of this diagram is automatically taken into account in the η-η' mixing angle; as a result, we neglect Fig. 2(b) henceforth. From Fig. 2(a) one can see that both pion emission (which must come from nonstrange quarks) and $\bar{K}$ emission (which must come from a strange quark) involve the creation of a nonstrange quark-antiquark pair. In these two cases our assumption of SU(3) symmetry would presumably be on an even better footing and since most of the data are on the channels $B'\pi$ and $B'\bar{K}$, this is comforting. Finally, on the question of SU(3) breaking, we mention that we have explicitly checked the effects of wave-function distortions in strange states due to the presence of the heavier strange quark.[5] While such effects are not always negligible, they are not as large as the discrepancies between theory and experiment encountered in the nonstrange sector; we therefore neglect them as being too fine a detail for our simple model.

While it is possible to consider a dynamical model for meson emission,[18] we take the simple approach here of approximating the mesons by pointlike structures and considering the amplitudes $q \to qM$. This point-like approximation can be supported by arguments from PCAC (partial conservation of axial-vector current).[21] In any event, in this approximation the meson-emission amplitude must be of the form

$$\langle B'(p's')M(K)|T|B(ps)\rangle = -\frac{3i}{(2\pi)^{3/2}}\langle B'(p's')|(g\vec{K}\cdot\vec{\sigma}_3+h\vec{\sigma}_3\cdot\vec{p}_3')e^{-i\vec{K}\cdot\vec{r}_3}X_3^M|B(ps)\rangle, \tag{5}$$

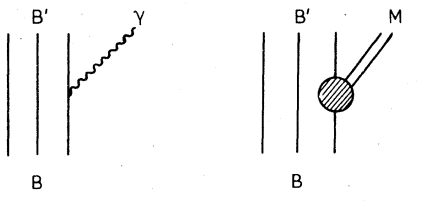

FIG. 1. (a) A baryon photon emission. (b) A baryon meson emission.

FIG. 2. (a) Okubo-Zweig-Iizuka (OZI) rule allowed meson emission. (b) OZI rule forbidden meson emission.

where g and h are two "elementary" emission amplitudes reflecting the dynamics of Fig. 2 and where X_3^M is the flavor operator for emission of meson M from the third quark with

$$X^{\pi^0}=\lambda_3,\quad X^{K^-}=(1/\sqrt{2})(\lambda_4+i\lambda_5),$$

$$X^{K^0}=\frac{-1}{\sqrt{2}}(\lambda_6-i\lambda_7),\quad X^{\eta}=\left(\frac{1+\sqrt{2}}{\sqrt{6}}\right)\lambda_8+\left(\frac{\sqrt{2}-1}{3}\right)\underline{1},$$

etc., in which the λ_i are the usual Gell-Mann matrices, and $\underline{1}$ is the 3×3 unit matrix. We have assumed the "perfect" mixing pattern for the η,[23]

$$\eta=\frac{1}{\sqrt{2}}(M_{\rm ns}-M_s)=\left(\frac{1+\sqrt{2}}{\sqrt{6}}\right)\eta_8+\left(\frac{\sqrt{2}-1}{\sqrt{6}}\right)\eta_1, \quad (6)$$

where $M_{\rm ns}\equiv(1/\sqrt{2})(u\bar{u}+d\bar{d})$ and $M_s=s\bar{s}$, in the above formula for X^η, corresponding to an η-η', mixing angle of $\sim -10^0$.

The calculation of the transition amplitudes (4) and (5) is most easily accomplished by choosing $\vec{K}$ along the $+\hat{z}$ direction. Apart from flavor and spin factors, this leads to integrals of the form

$$\int_0^\infty dx\, x^{\mu-1/2}e^{-\alpha^2x^2}j_{\nu-1/2}(\beta x)$$

$$=\frac{\pi^{1/2}}{2^{\nu+3/2}}\frac{\beta^{\nu-1/2}}{\alpha^{\mu+\nu}}\frac{\Gamma(\frac{1}{2}(\mu+\nu))}{\Gamma(\nu+1)}M\left(\frac{\mu+\nu}{2},\nu+1,-\frac{\beta^2}{4\alpha^2}\right), \quad (7)$$

where $M(a,b,c)=M(b-a,b,-c)e^{-c}$ is a confluent hypergeometric function which has the property that $M(b-a,b,-c)$ is a polynomial for all the cases considered here. In terms of the calculated helicity amplitudes $A_{s's}$, the partial widths are given by

$$\Gamma=\frac{1}{2J_R+1}\frac{KE'}{2\pi M_R}\sum_{s's}|A_{s's}|^2, \quad (8)$$

where J_R and M_R are the angular momentum and mass of the decaying resonance and s and s' are the initial and final spins defining a given helicity amplitude.

We will actually quote our amplitudes, not in the helicity basis, but in the conventional partial-wave basis; this basis is defined in subsection 6 of the Appendix. We find that apart from an overall strength factor, all of the states in a given SU(6)×O(3) multiplet share common partial-wave amplitudes independent of their flavor and total angular momentum J; e.g., $\Delta_{\frac{7}{2}}^{+}$ and $N_{\frac{3}{2}}^{+}$ of the $(56,2^+)$ share the same F-wave $N\pi$ amplitude. The sharing actually goes much further: The amplitudes which appear depend only on the total excitation quantum number N of the harmonic oscillator and the value of L^P, so that $(56,2^+)$ and $(70,2^+)$ decays are governed by the same amplitudes. These "universal" nonrelativistic amplitudes are displayed in Table I, from which one can see that the amplitudes fall into two classes. The first class, which we call "structure independent," consists of P_0, D, and F which have only the momentum dependence dictated by angular momentum considerations along with the gentle "elastic form factor" $e^{-(1/6)(K/\alpha)^2}$ The second class of amplitudes, consisting of

TABLE I. The universal partial-wave amplitudes for pseudoscalar emission to unmixed gound states. The full amplitudes denoted by the symbols in column two are obtained by multiplying column three by $\alpha\,[(K/\pi)(E'/M_R)]^{1/2}\exp[-\frac{1}{6}(K^2/\alpha^2)]$. For the definitions of G, G', G'', H', and H'' compare to Ref. 22.

Multiplet	Amplitude	Nonrelativistic model	Relativistic model
$(56,0^+)$	P_0	$[g-\frac{1}{3}h]\left(\frac{K}{\alpha}\right)$	G
$(70,1^-)$	S	$\left[(g-\frac{1}{3}h)\left(\frac{K}{\alpha}\right)^2+3h\right]$	$G'-3H'$
	D	$[g-\frac{1}{3}h]\left(\frac{K}{\alpha}\right)^2$	G'
$(56',0^+)$ and $(70,0^+)$	P_0'	$\left[(g-\frac{1}{3}h)\left(\frac{K}{\alpha}\right)^2+2h\right]\left(\frac{K}{\alpha}\right)$	$G''-2H''$
	F_0'	0	0
$(56,2^+)$ and $(70,2^+)$	P	$\left[(g-\frac{1}{3}h)\left(\frac{K}{\alpha}\right)^2+5h\right]\left(\frac{K}{\alpha}\right)$	$G''-5H''$
	F	$[g-\frac{1}{3}h]\left(\frac{K}{\alpha}\right)^3$	G''
$(20,1^+)$	P'	0	0
	F'	0	0

S, P'_0, and P we dub "structure dependent" as they, in addition to having the required momentum dependence of the first class of amplitudes, are polynomials in K/α which are highly sensitive to the structure of the states. We respond to this observation by taking an approach that is different from the usual one adopted in explicit quark models and *specifically forego attempting to calculate the structure-dependent amplitudes in terms of g and h*. In practice this means that our decay amplitudes, instead of being described by only the two parameters g and h, are described in terms of four. Recalling that our main objective here is to test the model for baryon structure, this relaxation of the decay model seems to us both sensible and prudent. The appearance of these two classes of amplitudes is a quite general feature of explicit decay models; in Table I we also show the closely analogous relativistic amplitudes obtained in the model of Feynman, Kislinger, and Ravndal.[22]

We have further chosen to represent the structure-dependent amplitudes by momentum-independent constants multiplying the standard angular momentum and $e^{-(1/6)(K/\alpha)^2}$ factor. This is done both for simplicity and because we believe that the emission of a real pion will tend to wash out any other momentum dependence of these amplitudes. The values of the reduced partial-wave amplitudes [i.e., the amplitudes in square brackets in Table I] which we use in our calculations are shown in Table II. From our photon amplitudes we find that $\alpha = 0.41$ GeV in accord with Copley, Karl, and Obryk.[19]

Before proceeding, we would like to mention an amusing feature of these amplitudes. If one had an exactly harmonic spectrum, then $(K/\alpha)_{N=2}$ would be approximately $2(K/\alpha)_{N=1} \equiv 2z$ and we would have

$$\tilde{P}_0 = \tilde{D} = \tilde{F} = [(g - \tfrac{1}{3}h)], \tag{9a}$$

$$\tilde{S} = [(g - \tfrac{1}{3}h)z^2 + 3h], \tag{9b}$$

$$\tilde{P} = [4(g - \tfrac{1}{3}h)z^2 + 5h], \tag{9c}$$

$$\tilde{P}'_0 = [4(g - \tfrac{1}{3}h)z^2 + 2h]. \tag{9d}$$

Thus, since $z \simeq 1$, for $(g - \frac{1}{3}h) = +5.7$ and $h = -3.4$ we would find $\tilde{P}_0 \simeq +6$, $\tilde{S} \simeq -5$, $\tilde{P} \simeq +6$, and $\tilde{P}'_0 \simeq +16$, not so dissimilar to the observed pattern. This example also has the nice feature that the counterparts of $(g - \frac{1}{3}h)$ and h automatically have opposite signs in the relativistic model of Ref. 22. However, since the actual multiplet spacing is rather far from harmonic and since there are large splittings even within multiplets, these considerations should only be considered illustrative.

TABLE II. The values of the reduced partial-wave amplitudes.

Reduced amplitude	Fitted value (GeV^{-1})
$\tilde{P}_0 = \tilde{D} = \tilde{F}$	+6
$\tilde{S}$	−7
$\tilde{P}$	+11
$\tilde{P}'_0$	+12

The actual calculations of amplitudes are straightforward. In the Appendix we have gathered together all of our wave functions and made all of our phase choices explicit in an attempt to enhance the usefulness of our compilation of amplitudes. In Tables III and IV we present amplitudes for γ and pseudoscalar meson transitions from states with up to two units of orbital angular momentum and up to one radial excitation in the harmonic oscillator model to the unmixed ground-state configuration. There are two circumstances in which we have chosen to extend the calculations beyond those outlined above. In certain special cases these amplitudes may be exactly zero as a result of SU(6) selection rules.[20,21] In other cases we will find amplitudes that are small for various dynamical reasons. It has been argued[24] that the observed violations of SU(6) selection rules are due to transitions into a color-hyperfine-interaction-induced admixture of ^2S_M [or (70,0*) in SU(6) language] configurations into the ground states. We have found that the resulting violations of SU(6) selection rules for pseudoscalar meson decays may be calculated in terms of the known amplitudes of Table II (see the first half of Table V). For meson decay amplitudes that turn out to be small for dynamical reasons, we have also studied the effects of ^2S_M configurations in the ground states. We find that these corrections are usually small, with the occasional exception in the case where the decaying state itself contains a significant ^2S_M or ^4S_M component; the relevant amplitudes in this case are shown in the second half of Table V. One can see from the table that unlike the SU(6)-violating amplitudes, these amplitudes are structure dependent and not calculable in terms of the parameters of Table II. Furthermore, their structure dependence would lead one to expect them to be smaller than P_0; we have accordingly neglected them in what follows. The explicit SU(6)-violating meson and photon amplitudes may be found in Table VI. The notation used in all of our tables has been developed previously[3,4,8] and is detailed in the Appendix. The actual strong decay amplitudes in Tables IV and VI are $\sigma_{\text{out}}\sqrt{\Gamma_{\text{out}}}$, while Tables VIII–XI will give

TABLE III. Photon-decay amplitudes. The full photon amplitudes are obtained by multiplying the entries in this table by the factor $(2\pi/K)^{1/2}\mu_p \exp[-\frac{1}{6}(K^2/\alpha^2)]$, where μ_p is the proton magnetic moment.

State	$A^p_{3/2}$	$A^p_{1/2}$	$A^n_{3/2}$	$A^n_{1/2}$
$\Delta(^4S_S)\frac{3}{2}^+$	$-\frac{2\sqrt{3}}{3}K$	$-\frac{2}{3}K$		
$N(^4P_M)\frac{5}{2}^-$	0	0	$-\frac{\sqrt{10}}{15}\frac{K^2}{\alpha}$	$-\frac{\sqrt{5}}{15}\frac{K^2}{\alpha}$
$N(^4P_M)\frac{3}{2}^-$	0	0	$+\frac{\sqrt{15}}{15}\frac{K^2}{\alpha}$	$+\frac{\sqrt{5}}{45}\frac{K^2}{\alpha}$
$N(^4P_M)\frac{1}{2}^-$		0		$+\frac{1}{9}\frac{K^2}{\alpha}$
$N(^2P_M)\frac{3}{2}^-$	$+\frac{\sqrt{6}}{3}\alpha$	$+\frac{\sqrt{2}}{3}\left(1-\frac{K^2}{\alpha^2}\right)\alpha$	$-\frac{\sqrt{6}}{3}\alpha$	$-\frac{\sqrt{2}}{3}\left(1-\frac{K^2}{3\alpha^2}\right)\alpha$
$N(^2P_M)\frac{1}{2}^-$		$+\frac{2}{3}\left(1+\frac{K^2}{2\alpha^2}\right)\alpha$		$-\frac{2}{3}\left(1+\frac{K^2}{6\alpha^2}\right)\alpha$
$\Delta(^2P_M)\frac{3}{2}^-$	$-\frac{\sqrt{6}}{3}\alpha$	$-\frac{\sqrt{2}}{3}\left(1+\frac{K^2}{3\alpha^2}\right)\alpha$		
$\Delta(^2P_M)\frac{1}{2}^-$		$-\frac{2}{3}\left(1-\frac{K^2}{6\alpha^2}\right)\alpha$		
$N(^2S'_S)\frac{1}{2}^+$		$-\frac{\sqrt{6}}{18}\frac{K^3}{\alpha^2}$		$+\frac{\sqrt{6}}{27}\frac{K^3}{\alpha^2}$
$\Delta(^4S'_S)\frac{3}{2}^+$	$+\frac{1}{9}\frac{K^3}{\alpha^2}$	$+\frac{\sqrt{3}}{27}\frac{K^3}{\alpha^2}$		
$N(^4S_M)\frac{3}{2}^+$	0	0	$+\frac{1}{18}\frac{K^3}{\alpha^2}$	$+\frac{\sqrt{3}}{54}\frac{K^3}{\alpha^2}$
$N(^2S_M)\frac{1}{2}^+$		$+\frac{\sqrt{3}}{18}\frac{K^3}{\alpha^2}$		$-\frac{\sqrt{3}}{54}\frac{K^3}{\alpha^2}$
$\Delta(^2S_M)\frac{1}{2}^+$		$+\frac{\sqrt{3}}{54}\frac{K^3}{\alpha^2}$		
$N(^2D_S)\frac{5}{2}^+$	$+\frac{2\sqrt{10}}{15}K$	$+\frac{2\sqrt{5}}{15}\left(1-\frac{K^2}{2\alpha^2}\right)K$	0	$+\frac{2\sqrt{5}}{45}\frac{K^3}{\alpha^2}$
$N(^2D_S)\frac{3}{2}^+$	$-\frac{\sqrt{10}}{15}K$	$+\frac{\sqrt{30}}{15}\left(1+\frac{K^2}{3\alpha^2}\right)K$	0	$-\frac{2\sqrt{30}}{135}\frac{K^3}{\alpha^2}$
$\Delta(^4D_S)\frac{7}{2}^+$	$+\frac{2\sqrt{7}}{63}\frac{K^3}{\alpha^2}$	$+\frac{2\sqrt{105}}{315}\frac{K^3}{\alpha^2}$		
$\Delta(^4D_S)\frac{5}{2}^+$	$-\frac{2\sqrt{35}}{105}\frac{K^3}{\alpha^2}$	$-\frac{\sqrt{70}}{315}\frac{K^3}{\alpha^2}$		
$\Delta(^4D_S)\frac{3}{2}^+$	$+\frac{\sqrt{10}}{45}\frac{K^3}{\alpha^2}$	$-\frac{\sqrt{30}}{135}\frac{K^3}{\alpha^2}$		
$\Delta(^4D_S)\frac{1}{2}^+$		$+\frac{\sqrt{30}}{135}\frac{K^3}{\alpha^2}$		
$N(^4D_M)\frac{7}{2}^+$	0	0	$+\frac{\sqrt{7}}{63}\frac{K^3}{\alpha^2}$	$+\frac{\sqrt{105}}{315}\frac{K^3}{\alpha^2}$
$N(^4D_M)\frac{5}{2}^+$	0	0	$-\frac{\sqrt{35}}{105}\frac{K^3}{\alpha^2}$	$-\frac{\sqrt{70}}{630}\frac{K^3}{\alpha^2}$
$N(^4D_M)\frac{3}{2}^+$	0	0	$+\frac{\sqrt{10}}{90}\frac{K^3}{\alpha^2}$	$-\frac{\sqrt{30}}{270}\frac{K^3}{\alpha^2}$
$N(^4D_M)\frac{1}{2}^+$		0		$+\frac{\sqrt{30}}{270}\frac{K^3}{\alpha^2}$
$N(^2D_M)\frac{5}{2}^+$	$-\frac{2\sqrt{5}}{15}K$	$-\frac{\sqrt{10}}{15}\left(1-\frac{K^2}{2\alpha^2}\right)K$	$+\frac{2\sqrt{5}}{15}K$	$+\frac{\sqrt{10}}{15}\left(1-\frac{K^2}{3\alpha^2}\right)K$
$N(^2D_M)\frac{3}{2}^+$	$+\frac{\sqrt{5}}{15}K$	$-\frac{\sqrt{15}}{15}\left(1+\frac{K^2}{3\alpha^2}\right)K$	$-\frac{\sqrt{5}}{15}K$	$+\frac{\sqrt{15}}{15}\left(1+\frac{K^2}{9\alpha^2}\right)K$
$\Delta(^2D_M)\frac{5}{2}^+$	$+\frac{2\sqrt{5}}{15}K$	$+\frac{\sqrt{10}}{15}\left(1+\frac{K^2}{6\alpha^2}\right)K$		
$\Delta(^2D_M)\frac{3}{2}^+$	$-\frac{\sqrt{5}}{15}K$	$+\frac{\sqrt{15}}{15}\left(1-\frac{K^2}{9\alpha^2}\right)K$		
$N(^2P_A)\frac{3}{2}^+$	0	0	0	0
$N(^2P_A)\frac{1}{2}^+$		0		0

TABLE IV. Pseudoscalar decay amplitudes. Amplitudes for pseudoscalar-octet decays may be taken from this table by the use of standard SU(3) isoscalar factors (see, e.g., the compilation of Ref. 25); for η decays use Eq. (6) and the relations $A(B_8^* \to B_8\eta_1) = \sqrt{2}A(N \to N\eta_8)$ and $A(B_{10}^* \to B_{10}\eta_1) = \sqrt{2}A(\Delta \to \Delta\eta_8)$. We have suppressed a factor of $+i$ in front of all P_M amplitudes.

State	$B_8 \to B_8M_8$ D type	$B_8 \to B_8M_8$ F type	$B_{10} \to B_8M_8$	$B_8 \to B_{10}M_8$	$B_{10} \to B_{10}M_8$	$B_1 \to B_8M_8$
$10\,^4S_S\,\frac{3}{2}^+$			$+\frac{2\sqrt{6}}{3}P_0$			
$8\,^4P_M\,\frac{5}{2}^-$	$-\frac{1}{3}D$	$+\frac{\sqrt{5}}{15}D$		$-\frac{\sqrt{14}}{6}D$		
$8\,^4P_M\,\frac{3}{2}^-$	$-\frac{\sqrt{6}}{18}D$	$+\frac{\sqrt{30}}{90}D$		$-\frac{5\sqrt{6}}{18}S, -\frac{2\sqrt{6}}{9}D$		
$8\,^4P_M\,\frac{1}{2}^-$	$+\frac{\sqrt{15}}{9}S$	$-\frac{\sqrt{3}}{9}S$		$-\frac{\sqrt{30}}{18}S$		
$8\,^2P_M\,\frac{3}{2}^-$	$+\frac{\sqrt{15}}{18}D$	$+\frac{5\sqrt{3}}{18}D$		$+\frac{\sqrt{15}}{9}S, -\frac{\sqrt{15}}{9}D$		
$8\,^2P_M\,\frac{1}{2}^-$	$+\frac{\sqrt{15}}{18}S$	$+\frac{5\sqrt{3}}{18}S$		$-\frac{\sqrt{30}}{9}S$		
$10\,^2P_M\,\frac{3}{2}^-$			$-\frac{\sqrt{3}}{9}D$		$+\frac{2\sqrt{6}}{9}S, \frac{-2\sqrt{6}}{9}D$	
$10\,^2P_M\,\frac{1}{2}^-$			$-\frac{\sqrt{3}}{9}S$		$-\frac{4\sqrt{3}}{9}S$	
$1\,^2P_M\,\frac{3}{2}^-$						$+\frac{\sqrt{6}}{3}D$
$1\,^2P_M\,\frac{1}{2}^-$						$+\frac{\sqrt{6}}{3}S$
$8\,^2D_S\,\frac{5}{2}^+$	$+\frac{1}{9}F$	$+\frac{2\sqrt{5}}{45}F$		$-\frac{\sqrt{30}}{45}P, +\frac{2\sqrt{5}}{45}F$		
$8\,^2D_S\,\frac{3}{2}^+$	$+\frac{1}{9}P$	$+\frac{2\sqrt{5}}{45}P$		$-\frac{\sqrt{5}}{45}P, +\frac{\sqrt{5}}{15}F$		
$10\,^4D_S\,\frac{7}{2}^+$			$+\frac{2\sqrt{35}}{105}F$		$+\frac{\sqrt{210}}{105}F$	
$10\,^4D_S\,\frac{5}{2}^+$			$+\frac{2\sqrt{70}}{135}F$		$+\frac{\sqrt{42}}{45}P, +\frac{16\sqrt{7}}{315}F$	
$10\,^4D_S\,\frac{3}{2}^+$			$-\frac{2\sqrt{5}}{45}P$		$+\frac{4\sqrt{2}}{45}P, +\frac{\sqrt{2}}{15}F$	
$10\,^4D_S\,\frac{1}{2}^+$			$-\frac{2\sqrt{10}}{45}P$		$+\frac{\sqrt{10}}{45}P$	
$8\,^2S'_S\,\frac{1}{2}^+$	$+\frac{\sqrt{10}}{18}P'_0$	$+\frac{\sqrt{2}}{9}P'_0$		$+\frac{\sqrt{5}}{9}P'_0$		
$10\,^4S'_S\,\frac{3}{2}^+$			$+\frac{\sqrt{2}}{9}P'_0$		$+\frac{\sqrt{5}}{9}P'_0, 0F'_0$	
$8\,^4S_M\,\frac{3}{2}^+$	$+\frac{\sqrt{10}}{36}P'_0$	$-\frac{\sqrt{2}}{36}P'_0$		$+\frac{5\sqrt{2}}{36}P'_0, \quad 0F'_0$		
$8\,^2S_M\,\frac{1}{2}^+$	$-\frac{\sqrt{5}}{36}P'_0$	$-\frac{5}{36}P'_0$		$+\frac{\sqrt{10}}{18}P'_0$		
$10\,^2S_M\,\frac{1}{2}^+$			$+\frac{1}{18}P'_0$		$+\frac{2}{9}P'_0$	
$1\,^2S_M\,\frac{1}{2}^+$						$-\frac{\sqrt{2}}{6}P'_0$
$8\,^4D_M\,\frac{7}{2}^+$	$+\frac{\sqrt{7}}{42}F$	$-\frac{\sqrt{35}}{210}F$		$+\frac{\sqrt{21}}{42}F$		
$8\,^4D_M\,\frac{5}{2}^+$	$+\frac{\sqrt{14}}{126}F$	$-\frac{\sqrt{70}}{630}F$		$+\frac{\sqrt{105}}{90}P, +\frac{4\sqrt{70}}{315}F$		
$8\,^4D_M\,\frac{3}{2}^+$	$-\frac{1}{18}P$	$+\frac{\sqrt{5}}{90}P$		$+\frac{2\sqrt{5}}{45}P, +\frac{\sqrt{5}}{30}F$		
$8\,^4D_M\,\frac{1}{2}^+$	$-\frac{\sqrt{2}}{18}P$	$+\frac{\sqrt{10}}{90}P$		$+\frac{1}{18}P$		
$8\,^2D_M\,\frac{5}{2}^+$	$-\frac{\sqrt{2}}{36}F$	$-\frac{\sqrt{10}}{36}F$		$-\frac{\sqrt{15}}{45}P, +\frac{\sqrt{10}}{45}F$		
$8\,^2D_M\,\frac{3}{2}^+$	$-\frac{\sqrt{2}}{36}P$	$-\frac{\sqrt{10}}{36}P$		$-\frac{\sqrt{10}}{90}P, +\frac{\sqrt{10}}{30}F$		

TABLE IV. *(Continued.)*

State	$B_8 \to B_8 M_8$ *D* type	$B_8 \to B_8 M_8$ *F* type	$B_{10} \to B_8 M_8$	$B_8 \to B_{10} M_8$	$B_{10} \to B_{10} M_8$	$B_1 \to B_8 M_8$
$10\,^2D_M\frac{5^+}{2}$			$+\frac{\sqrt{10}}{90}F$		$-\frac{2\sqrt{6}}{45}P, +\frac{4}{45}F$	
$10\,^2D_M\frac{3^+}{2}$			$+\frac{\sqrt{10}}{90}P$		$-\frac{2}{45}P, +\frac{2}{15}F$	
$1\,^2D_M\frac{5^+}{2}$						$-\frac{\sqrt{5}}{15}F$
$1\,^2D_M\frac{3^+}{2}$						$-\frac{\sqrt{5}}{15}P$
$8\,^2P_A\frac{3^+}{2}$	$0P'$	$0P'$		$0P', 0F'$		
$8\,^2P_A\frac{1^+}{2}$	$0P'$	$0P'$		$0P'$		
$1\,^4P_A\frac{5^+}{2}$						$0P'$
$1\,^4P_A\frac{3^+}{2}$						$0P'$
$1\,^4P_A\frac{1^+}{2}$						$0P'$

TABLE V. Some universal partial-wave amplitudes for pseudoscalar emission to impurities in the ground states. The full amplitudes denoted by the symbols in column three are obtained by multiplying column four by $\alpha\,[(K/\pi)\,(E'/M_R)^{1/2}\exp[-\frac{1}{6}(K^2/\alpha^2)]$.

Initial state		Final state	Amplitude	Nonrelativistic model
$\Lambda_8\,^4P_M$	$\to$	$N\,^2S_M$	D_{70} (=D)	$[g-\frac{1}{3}h]\left(\frac{K}{\alpha}\right)^2$
$N\,^4P_M$	$\to$	$\Lambda_8\,^2S_M$	D_{70} (=D)	$[g-\frac{1}{3}h]\left(\frac{K}{\alpha}\right)^2$
	$\to$	$\Lambda_1\,^2S_M$	D_{70} (=D)	$[g-\frac{1}{3}h]\left(\frac{K}{\alpha}\right)^2$
$\Lambda_8\,^4D_M$	$\to$	$N\,^2S_M$	F_{70} (=F)	$[g-\frac{1}{3}h]\left(\frac{K}{\alpha}\right)^3$
$N\,^4D_M$	$\to$	$\Lambda_8\,^2S_M$	F_{70} (=F)	$[g-\frac{1}{3}h]\left(\frac{K}{\alpha}\right)^3$
	$\to$	$\Lambda_1\,^2S_M$	F_{70} (=F)	$[g-\frac{1}{3}h]\left(\frac{K}{\alpha}\right)^3$
$\Lambda_8\,^4S_M$	$\to$	$N\,^2S_M$	P^a_{70}	$\left[(g-\frac{1}{3}h)\left(1-\frac{K^2}{9\alpha^2}\right)\right]\left(\frac{K}{\alpha}\right)$
$\Lambda_8\,^2S_M$	$\to$	$N\,^2S_M$	P^b_{70}	$\left[(g-\frac{1}{3}h)\left(1-\frac{K^2}{9\alpha^2}+\frac{K^4}{36\alpha^4}\right)\right]\left(\frac{K}{\alpha}\right)$
$N\,^4S_M$	$\to$	$N\,^2S_M$	P^c_{70}	$\left[(g-\frac{1}{3}h)\left(1-\frac{K^2}{9\alpha^2}+\frac{K^4}{216\alpha^2}\right)\right]\left(\frac{K}{\alpha}\right)$
$N\,^2S_M$	$\to$	$N\,^2S_M$	P^d_{70}	$\left[(g-\frac{1}{3}h)\left(1-\frac{K^2}{6\alpha^2}+\frac{7K^4}{72\alpha^2}\right)\right]\left(\frac{K}{\alpha}\right)$
$\Delta\,^2S_M$	$\to$	$N\,^2S_M$	P^e_{70}	$\left[(g-\frac{1}{3}h)\left(1-\frac{K^2}{9\alpha^2}+\frac{K^4}{216\alpha^2}\right)\right]\left(\frac{K}{\alpha}\right)$
$\Sigma_8\,^4S_M$	$\to$	$N\,^2S_M$	P^e_{70}	$\left[(g-\frac{1}{3}h)\left(1-\frac{K^2}{9\alpha^2}+\frac{K^4}{54\alpha^2}\right)\right]\left(\frac{K}{\alpha}\right)$
$\Sigma_8\,^2S_M$	$\to$	$N\,^2S_M$	P^e_{70}	$\left[(g-\frac{1}{3}h)\left(1-\frac{K^2}{9\alpha^2}+\frac{K^4}{216\alpha^2}\right)\right]\left(\frac{K}{\alpha}\right)$
$\Sigma_{10}\,^2S_M$	$\to$	$N\,^2S_M$	P^e_{70}	$\left[(g-\frac{1}{3}h)\left(1-\frac{K^2}{9\alpha^2}+\frac{K^4}{216\alpha^2}\right)\right]\left(\frac{K}{\alpha}\right)$

TABLE VI. Amplitudes of some SU(6)-violating processes. We have suppressed a factor of $+i$ in front of all P_M amplitudes; note also that the full photon amplitudes are obtained from these by multiplying by the factor $(2\pi/K)^{1/2}\mu_p \exp[-\frac{1}{6}(K^2/\alpha^2)]$, where μ_p is the proton magnetic moment.

Process	Amplitude
$N^4P_M\frac{5}{2}^- \to p^2S_M\frac{1}{2}^+ \gamma$	$A^p_{3/2} = -\frac{2\sqrt{15}}{45}\frac{K^2}{\alpha}, A^p_{1/2} = -\frac{\sqrt{30}}{45}\frac{K^2}{\alpha}$
$N^4D_M\frac{7}{2}^+ \to p^2S_M\frac{1}{2}^+ \gamma$	$A^p_{3/2} = -\frac{2\sqrt{42}}{189}\frac{K^3}{\alpha^2}, A^p_{1/2} = -\frac{2\sqrt{70}}{315}\frac{K^3}{\alpha^2}$
$\Lambda_8{}^4P_M\frac{5}{2}^- \to N^2S_M\frac{1}{2}^+ \bar{K}$	$+\frac{2\sqrt{15}}{45}D$
$\Lambda_8{}^4D_M\frac{7}{2}^+ \to N^2S_M\frac{1}{2}^+ \bar{K}$	$+\frac{2\sqrt{105}}{315}F$
$N^4P_M\frac{5}{2}^- \to \Lambda_8{}^2S_M\frac{1}{2}^+ K$	$+\frac{\sqrt{30}}{45}D$
$\to \Lambda_1{}^2S_M\frac{1}{2}^+ K$	$-\frac{\sqrt{30}}{45}D$
$N^4D_M\frac{7}{2}^+ \to \Lambda_8{}^2S_M\frac{1}{2}^+ K$	$+\frac{\sqrt{210}}{315}F$
$\to \Lambda_1{}^2S_M\frac{1}{2}^+ K$	$-\frac{\sqrt{210}}{315}F$

the numerical values of $\sigma_{in}\sigma_{out}\sqrt{\Gamma_{out}}$, where $\sigma_{in(out)}$ is the sign of the ingoing (outgoing) amplitude and Γ_{out} is the partial width of the outgoing decay channel.

IV. COMPARISON TO EXPERIMENT AND CONCLUSIONS

To compare to experiment[25,26,27] we simply combine the decay amplitudes of Sec. III with the baryon compositions of the model described in Sec. II. The ground-state compositions have not been quoted elsewhere and so are given in the Appendix. The P-wave and positive-parity baryon compositions have been published,[3,4] but in conventions which differ somewhat from those used here, so in the Appendix we also provide a short dictionary for translating these compositions into our present "standard" conventions.

The results of the calculation are shown in Tables VII–XI. For each predicted resonance (we use the standard partial-wave notation $L_{2I,2J}$ for $S=0$ states and $L_{I,2J}$ for $S=-1$ states) we show the theoretical mass and amplitudes while just underneath we give the experimental mass of the resonance we interpret as corresponding to the theoretical one and its amplitudes. We have usually not calculated rare amplitudes (ΞK, $\Delta\bar{K}$, $\Sigma^*\pi$, $N\gamma$, etc.) for weak or unseen resonances; when required they may be constructed from the tables of the preceding section.

For the most part we believe that the tables speak for themselves. They argue convincingly that at least the main features of baryon physics have been captured by the structure and decay models described here. The tables are so detailed, however, that it is perhaps worthwhile for us to try to summarize our findings.

The first feature we would like to emphasize is that the model explains the apparent absence of many predicted states from the partial-wave analyses; usually they are far too inelastic to be readily seen. This is illustrated in the case of the positive-parity excited baryons (similar effects occur in the negative-parity states) in Figs. 3 and 4 which compare the observed resonances (denoted by open boxes representing the regions in which the masses of the resonances most likely lie[25,26]) with predicted resonances represented by bars whose lengths indicate their visibility relative to the strongest resonance in the partial wave. These diagrams illustrate that the "problem" of missing states is not a problem—the states are only weakly coupled and should eventually be seen. One of the best examples of this is in the $\Lambda\frac{3}{2}^+$ sector where only one of the seven predicted resonances couples significantly to $N\bar{K}$. This result has a very simple interpretation, first discussed in Refs. 2, 3, and 4: The presence of the heavier strange quark causes a segregation of states into those in which the two nonstrange quarks oscillate and those in which the strange quark oscillates against the nonstrange pair. This leads naturally to the introduction of the "*uds* basis" and the classification of states as ρ (nonstrange) and λ (strange) oscillations; the former trivially decouple from $N\bar{K}$ and related channels in the single-quark transition picture.[28] In addition to confirming the decouplings that could be seen easily in the *uds* basis, this calculation reveals further extensive decouplings in the $S=-1$ states (especially in the Σ's) that yield the full results of Fig. 4. Equally remarkable are the results of the calculation for decouplings in the $S=0$ sector. The $N\frac{3}{2}^+$ states serve as an example equally striking to $\Lambda\frac{3}{2}^+$—even if less immediately interpretable. The five states predicted in this channel have elastic branching ratios predicted to be roughly in the ratio 1.0 : 0.16 : 0.01 : 0.01 : 0.00 (see the caption to Fig. 3 for a description of how these branching ratios have been estimated) indicating that only the lowest state should be readily observed, as is the case. We stress that in view of the coupling/decoupling picture shown in the figures, it seems reasonable to conclude that the complete baryon spectrum anticipated by the naive nonrelativistic quark model is present and that there is no need

TABLE VII. Photon amplitudes (theory versus experiment). The experimental numbers quoted are rough averages of the available data including not only the values listed by the Particle Data Group (PDG) (Ref. 25) but also more recent results (Ref. 26). The experimental values are given under the theoretical values.

State	Mass (MeV)	$A^p_{3/2}$	$A^p_{1/2}$	$A^n_{3/2}$	$A^n_{1/2}$
$P33$****	1240	−179	−103		
	1230–1235	−255 ± 10	−140 ± 5		
$D15$****	1670	+16 [a]	+12 [a]	−53	−37
	1650–1685	+20 ± 10	+15 ± 10	−60 ± 20	−50 ± 20
$D13$****	1535	+128	−23	−122	−45
	1510–1530	+165 ± 20	−15 ± 10	−130 ± 20	−70 ± 20
$D13$***	1745	+11	−7	−76	−15
	1660–1710	−10 ± 15	−15 ± 15	(+)40 ± 40	(+)30 ± 40
$S11$****	1490		+147		−119
	1500–1545		+65 ± 20		−60 ± 35
$S11$****	1655		+88		−35 [b]
	1660–1700		+50 ± 20		−50 ± 25
$D33$***	1685	+105	+100		
	1620–1720	+100 ± 25	+100 ± 30		
$S31$****	1685		+59		
	1600–1695		(+)40 ± 25		
$F17$**	1955	−10 [a]	−8 [a]	−23	−18
	1970–2000	0 ± ?	+25 ± ?	−70 ± ?	−85 ± ?
$F15$****	1715	+91	~0	−25 [b]	+26
	1670–1690	+125 ± 25	−10 ± 10	−30 ± 15	+30 ± 10
$P13$***	1710	+46	−133	−10	+57
	1650–1750	−35 ± 30	+50 ± 50	±50 ± 30	±15 ± 25
$P11$****	1405		−24		+16
	1390–1470		−70 ± 25		+40 ± 20
$P11$***	1705		−47		−21
	1650–1750		+45 ± 25		±30 ± 25
$F37$****	1915	−69	−50		
	1910–1950	−70 ± 20	−60 ± 20		
$F35$****	1940	−33	+8 [b]		
	1860–1910	−35 ± 20	+30 ± 20		
$P33$***	1780	−46	−16		
	1650–1900	−10 ± 40	0 ± 30		
$P31$****	1925		~0		
	1780–1960		−20 ± 20		

[a] SU(6) violations due to impurities in the ground state; see Ref. 24.
[b] Sign change due to mixing.

for schemes to eliminate, for example, the 70-even SU(6) supermultiplets.[29] Of course, the figures show much more: They show that in addition, the dynamics of the quark model of Sec. II predicts those states that do couple to be near their observed masses.

This last observation leads us to examine the details of the amplitudes more closely. To some extent the success of the model in predicting the signs and magnitudes of the decay amplitudes—especially with our method of dealing with the "structure-dependent" amplitudes—is simply reflecting the well-established success of the $SU(6)_W$ decay scheme.[21] In view of this it is probably worthwhile mentioning some of the ways in which our model is being tested beyond this level:

(1) The $SU(6)_W$ model does not, of course, predict where the resonances whose decays it fits will be found, nor what their structures will be. As mentioned in the Introduction this becomes especially important when the complexity of possible mixings increases—as it soon does—to the point where $SU(6)_W$ loses its predictive power (unless it makes *ad hoc* assumptions on mixing angles).

(2) Even with the "structure-dependent" amplitudes, our scheme successfully relates decays in different multiplets while $SU(6)_W$ cannot. We have not only the very nice relation $\tilde{P}_0 = \tilde{D} = \tilde{F}$ between the structure-independent amplitudes, but also it should be noted that $\tilde{P}$ and $\tilde{F}$ are amplitudes common to both the $(56, 2^+)$ and $(70, 2^+)$ supermultiplets, and that $\tilde{P}'_0$ is common to

TABLE VIII. N pseudoscalar decays (theory versus experiment). See caption to Table VII.

State	Mass (MeV)	$N\pi$	$N\eta$	ΣK	ΛK	$\Delta\pi$	Comments
$D15$****	1670	5.5	−2.8	−small	+0.1	−9.3	
	1650–1685	8.3 ± 1	(−)1 ± 1	<±0.05	<±0.6	−8.7 ± 1	
$D13$****	1535	9.2	+0.4	no	no	S:+6.7 D:+2.5	
	1510–1530	8.3 ± 1	+0.4 ± 0.2			S:+3.9 ± 1 D:+3.8 ± 1	
$D13$***	1745	3.6	−0.7	−small	−0.2	S:+16 D:−7.7	
	1660–1710	3.5 ± 1	±2 ± 1	<±0.7	±1 ±1	S:(+)5 ±5 D:±4.2 ± 2	
$S11$****	1490	5.3	+5.2	no	no	−1.7	
	1500–1545	5.5 ± 2	+8.1 ± 1			(−)1.1 ± 1	
$S11$****	1655	8.7	−1.5	≃−2	−3.0	−8.2	
	1660–1700	9.1 ± 1	(−)1.6 ± 1	±2.5 ± 1	−4.0 ± 1	−3.6 ± 1	
$F17$**(*)	1955	3.1	−2.3	−1.7	−0.3	−6.0	
	1970–2000	4.5 ± 2	(−)2 ±2	±1.5 ± 1.5	(−)1 ±2		
$F15$****	1715	7.1	+0.7	−small	−0.1	P:+2.0 F:−0.7	
	1670–1690	9.2 ± 1	±0.3 ± 0.2	<±0.02	(−)0.2 ± 0.2	P:+3.9 ± 1 F:−1.0 ± 1	
$F15$ not seen	1955	0.4			−3.2	P:+4.7 F:−6.5	weak $N\pi$, very inelastic to $\Delta\pi$
$F15$**	2025	1.3	−0.6	−0.7	+0.9	P:−7.0 F:−4.3	
	1970–2025	4.7 ± 2		±1 ±1			
$P13$***	1710	6.5	+1.9	+small	−1.7	P:+1.9 F:−1.0	
	1650–1750	6.3 ± 2	(−)3 ±2	±2.2 ± 1	−2.5 ± 1	P:(+)5.4 ± 1 F:?	
$P13$ not seen	1870	3.2	−2.9	−3.3		P:−4.1 F:−1.5	
$P13$ not seen	1955	1.1				P:−9.4 F:−0.7	very inelastic to $(\Delta\pi)_P$
$P13$ not seen	1980	1.1				P:−3.4 F:+9.2	weak $N\pi$, very inelastic to $(\Delta\pi)_F$
$P13$ not seen	2060	0.5				P:+3.4 F:+4.5	decouples from $N\pi$
$P11$****	1405	6.8	+small	no	−small	−2.4	*ΛK signs from extrapolation to below threshold
	1390–1470	11 ±2	+5 ±3(?)		−*	−6.4 ± 2	$N\eta$ experimental amplitude correlated with $P11(1780)$
$P11$***	1705	6.7	+2.9	+0.8	−2.1	+3.6	
	1650–1750	5.7 ± 2	(+)4 ±2	±4 ±2	−2.8 ± 1	(+)4.8 ± 1	
$P11$ not seen	1890	4.4	−0.8	−1.7	−1.4	+3.4	relatively inelastic to $N\pi$
$P11$ not seen	2055	1.2				+1.8	very weak πN

TABLE IX. Δ pseudoscalar decays (theory versus experiment). See caption to Table VII.

State	Mass (MeV)	$N\pi$	ΣK	$\Delta\pi$		Comments
$P33$****	1240	11	no	no		
	1230–1235	11 ±1				
$D33$***	1685	4.9	−small	S:−10.3	D:−6.3	
	1620–1720	6.7 ±1	±0.4 ±0.4	S:−9.7 ±1	D:−2.5 ±1	
$S31$****	1685	3.3	−small	+8.0		
	1600–1695	5.5 ±1		+8.4 ±1		
$F37$****	1915	7.5	−1.9	F:−5.5	H:0.0	
	1910–1950	9.8 ±1	±2 ±1	F:(−)6.7 ±1	H:small	
$F35$****	1940	4.0	−0.8	P:−3.2	F:−5.5	
	1860–1910	6.1 ±2	±2 ±1	P:small	F:(−)6.6 ±2	
$F35$ not seen	1975	1.0		P:6.2	F:−1.4	weak πN coupling
$P33$	1780 (theory)	5.4	−1.9	P:−8.6	F:−0.1	PDG comments Δ(1690)
***	1650–1950 (expt)	6.1 ±2	±0.8 ±0.8	P:−11 ±2	F:(+)2 ±1	may include more than
$P33$	1925 (theory)	5.2	−3.2	P:+3.2	F:+1.4	one resonance; see also Ref. 26
$P33$ not seen	1975	0.1		P:+0.5	F:−7.7	decouples from πN
$P31$	1875 (theory)	2.7	−1.3	+7.6		
***	1780–1960 (expt)	6.6 ±2	±3.6 ±1	(−)2 ±1		
$P31$	1925 (theory)	5.3	−3.4	−5.9		

$(56', 0^+)$ and $(70, 0^+)$.

(3) Next we would like to try to highlight those features of our results which provide some evidence for the QCD-like components of the quark model of Sec. II. The purely spectroscopic evidence has been discussed in Refs. 1–11, so here we concentrate only on the evidence from the decay amplitudes. In general, these amplitudes show that the spectroscopic successes of the model are not accidental in that the coincidences between theoretical and experimental masses are substantiated by coinciding theoretical and experimental internal structures for the states. We have already mentioned the *uds* basis and the extensive decouplings in the $S=-1$ sector which result from the dynamical segregation of states into "ρ"- and "λ"-type states. This segregation indicates that the confinement is flavor independent, as this is the main assumption on which it is based, supporting the idea that flavor-symmetry breaking is entirely due to the quark mass differences. In addition to this "confinement mixing" of states, the hyperfine interactions also produce very important mixing effects:

(a) In the $N\frac{1}{2}^-$ sector in the absence of mixing the $N(1700)$ would have twice the $N\eta$ width of the $N(1535)$; with the mixing its $N\eta$ width is predicted to be ten times smaller as observed. These mixings also produce substantial effects in the strange states and in photon decays; for example, the large value of $A^p_{3/2}$ for $S11(1700)$ is entirely due to mixing. As explained in Refs. 1, 3, and 8 these successes indicate that the tensor piece of the hyperfine interaction (3) is present with the expected sign and strength relative to the contract term.

(b) Hyperfine interactions produce extensive mixing between the $(56, 2^+)$ and $(70, 2^+)$ multiplets which has several important effects. In the $N\frac{5}{2}^+$ sector it predicts that N(1688) will be much more strongly coupled to $N\pi$ than the two higher resonances in this channel, as observed; the unmixed $N\,^2D_S$ and $N\,^2D_M$ would have had about equal couplings. A similar effect occurs in the $\Delta\frac{5}{2}^+$ sector.[30] Here the strong ^4D_S-^2D_M tensor mixing essentially decouples the upper state from $N\pi$ (only one state is seen) while it produces an otherwise unexpected dominant F-wave $\Delta\pi$ decay of the Δ(1890) as observed. We have already mentioned the $N\frac{3}{2}^+$ sector in praise of its decoupling properties. These are also partly due to $(56, 2^+)$-$(70, 2^+)$ mixing as once again the unmixed $N\,^2D_S$ and $N\,^2D_M$ would have had $N\pi$ couplings of about the same strength. Similar effects, sometimes partially masked by the ρ-λ effect, are present in the $S=-1$ sector as well. As an example of the effects of the mixing on photon decays, we mention the $F15(1688)$ where the $A^n_{3/2}$ amplitude arises entirely from mixing which, at the same time, leaves undisturbed the famous near-zero in the $A^p_{1/2}$ amplitude.[19]

(c) The tensor interaction also produces mixing of $L=0$ and $L=2$ states. The neatest example of this is in the $\Delta\frac{1}{2}^+$ sector where there is almost 50-50 mixing of ^2S_M and ^4D_S which essentially decouples one state from $N\pi$ and leaves the other

TABLE X. Λ pseudoscalar decays (theory versus experiment). See caption to Table VII.

State	Mass (MeV)	$N\bar{K}$	$\Sigma\pi$	$\Lambda\eta$	$\Sigma^*\pi$		Comments
$D05$****	1815	1.5	−7.7	−2.3	D:−7.8	G:0.0	
	1810–1830	2 ±1	−7 ±2	(−)2±1	D:±5±2	G:<±1	
$D03$****	1490	3.0	+2.8	no	S:+ small	D:+ small	$\Sigma^*\pi$ partial width
	1520±2	2.7±0.2	(+)2.6±0.2				~1 MeV
$D03$****	1690	4.3	−6.6	+0.1	S:+5.5	D:+2.3	
	1690±10	3.9±0.4	−4.3±0.3	±0.3±0.2	S:(+)4.2±0.6	D: ?	
$D03$ not seen	1880	1.1	−5.3		S:+14	D:−7.7	weakly coupled to $\bar{K}N$ very inelastic
$S01$****	1490	no	+7.4	no	no		
	1405±5		±6.1±0.4				
$S01$****	1650	3.3	−3.2	+2.2	−1.2		
	1660–1680	2.8±0.3	−4.4±0.4	(+)2.8±0.7	(−)2.5±0.7		
$S01$***	1800	2.9	−11	−3.9	−5.5		
	1700–1850	7 ±4	−5 ±3(?)		(−)1.4±1.0		
$F07$*(*)	2070	1.7	+4.0	+1.9	+4.1		
	2020–2120	2.6±1	(−)8 ±3				
$F05$****	1815	6.4	−2.0	−0.7	P:+1.5	F:−0.5	
	1820±5	6.9±0.7	−3.4±0.4	(−)1.2±0.5	P:+2.4±0.6	F:(−)0.8±0.4	
$F05$ ***	2010 (theory)	1.8	+7.4	−1.6	P:+0.4	F:−0.4	
	2050–2150 (expt)	4 ±2	+4 ±2		P:(−)2±1	F:<±1	
$F05$	2095 (theory)	1.7	+5.4	+0.9	P:−3.2	F:+6.2	
$F05$ not seen	2130	0.9	−0.3				almost decoupled from $\bar{K}N$
$F05$ not seen	2160	0.5	+1.6				almost decoupled from $\bar{K}N$
$P03$***	1810	7.4	−2.1	−1.8	P:−0.1	F:−1.1	
	1850–1920	5 ±3	±2.4±0.6		P:<±0.6	F:(+)2.5±1.0	
$P03$ not seen	1960	1.0	+2.0		P:−2.1	F:+0.1	almost decoupled from $\bar{K}N$
$P03$ not seen	2005	0.3	−7.4				decoupled from $\bar{K}N$
$P03$ not seen	2080	0.4	+0.1				decoupled from $\bar{K}N$
$P03$ not seen	2110	0.3	+2.4				decoupled from $\bar{K}N$
$P03$ not seen	2145	1.3	+2.7		P:−1.0	F:+4.0	almost decoupled from $\bar{K}N$
$P03$ not seen	2175	0.4	−0.2				decoupled from $\bar{K}N$
$P01$**	1555	5.4	−3.8	−small	−2.1		
	1570–1620	5±3	−5±3				
$P01$ **	1740 (theory)	5.7	+6.0	−1.3	+1.6		
	1750–1850 (expt)	6 ±3	±4 ±2		(+)0.5±1		
$P01$	1860 (theory)	4.6	−3.8	+0.7	+4.2		
$P01$ not seen	2020	1.8	−4.0	−1.3	+2.4		almost decoupled from $\bar{K}N$
$P01$ not seen	2175	0.6	−1.8				decoupled from $\bar{K}N$
$P01$ not seen	2205	0.0	0.0				decoupled from $\bar{K}N$

TABLE XI. Σ pseudoscalar decays (theory versus experiment). See caption to Table VII.

State	Mass (MeV)	$N\bar{K}$	$\Sigma\pi$	$\Lambda\pi$	$\Sigma^*\pi$	$\Delta\bar{K}$	Comments
$P13$****	1390	no	−2.8	+6.6	no	no	
	1385 ± 5		±2.1 ± 0.3	(+)5.7 ± 0.4			
$D15$****	1760	6.7	+3.0	−4.7	D:+2.9 D:+3.2 ± 0.4 G:0.0 G:<±0.5		
	1775 ± 10	7 ±1	+1.5 ± 0.3	−4.3 ± 0.6			
$D13$****	1675	2.1	+6.6	+2.4	S:+0.9 S:(+)2.5 ± 1.5 D:+0.5 D: ?		
	1675 ± 10	2.1 ± 1.1	+4.6 ± 2.3	+2.3 ± 1.0			
$D13$ not seen	1805	0.3	+3.9	−3.4	S:+2.5 D:+5.5		decoupled from $\bar{K}N$
$D13$***	1815	4.3	−4.0	−0.4	S:−11 S:(−)3 ± 2 D:−1.7 D:<±1.5	S:+6.2 S:(+)7 ± 3 D:−6.0 D:(+)7 ± 3	$\Delta\bar{K}$ signs are measured relative to $F17(2030)$
	1860–1950	4 ±3	(−)4 ±2	−3 ±1			
$S11$**	1650	5.3	+9.9	0.0	−0.1		
	1610–1635	2.5 ± 1.0	±4.5 ± 2	±4 ±2			
$S11$ *** $S11$	1750 (theory) 1730–1820 (expt) 1810 (theory)	4.1 4 ±2 2.5	−0.5 ±2 ±1 −4.1	−5.3 −2.8 ± 1.0 +0.5	+0.4 (+)4 ±3 +7.4		$\Sigma\eta$: −1.8, ±5 ± 2, −3.1
$F17$****	2015	5.4	−2.2	+3.2	F:−2.1 F:(−)4.4 ± 1.5 H:0.0 H:<±1	F:−3.8 F:−4 ± 2 H:0.0 H:<0.5	ΞK: −0.6, −0.6 ± 0.3; note ΞK and $\Delta\bar{K}$ sign conventional and opposite to Litchfield (Ref. 27)
	2020–2040	5.9 ± 1.1	−2.9 ± 1.5	+5.8 ± 1.1			
$F17$ not seen	2115	1.8	+4.1	−5.4	F:+4.5 H:0.0		relatively weak to $\bar{K}N$
$F15$****	1940	1.1	−5.3	−3.3	P:−0.8 P:<0.3 F:+0.5 F:(−)1.2 ± 0.5		
	1905–1930	3 ±1	−4 ±2	−3 ±1			
$F15$ * $F15$	2035 (theory) 2050–2100 (expt) 2060 (theory)	2.9 1.2	−0.2 +large +4.3	+1.9 −0.1	P:−2.7 F:−2.3 P:−1.1 F:+2.2		
$F15$ not seen	2105	0.6	−0.1	+3.0	P:+3.4 F:−3.3		weakly coupled to $\bar{K}N$
$F15$ not seen	2160	1.3	+1.8	−2.4	P:+4.8 F:+4.1		weakly coupled to $\bar{K}N$
$P13$*	1865	3.9	−2.1	+3.3	P:−8.2		
	1800–1850	7 ±2	(−)2 ±2	+2 ±2			
$P13$ not seen	1935	0.8	−5.6	−2.1	P:−1.4		weakly coupled to $\bar{K}N$
$P13$ $P13$ ** $P13$	2005 (theory) 2045 (theory) 2070–2130 (expt) 2080 (theory)	4.3 0.3 1.1	+0.7 +4.0 −0.6	−0.1 −3.9 (−)? −2.4	P:+3.6 P:+1.6 P:+5.3		
$P13$ not seen	2100	0.1	−1.0	+3.1	P:+2.0		decoupled from $\bar{K}N$
$P13$ not seen	2120	0.0	−1.3	+0.4	P:−0.8		decoupled from $\bar{K}N$
$P13$ not seen	2165	0.5	+1.1	−1.0	P:−2.1		decoupled from $\bar{K}N$
$P11$***	1640	1.2	−3.7	−2.9	+1.5		
	1580–1690	3 ±2	−6 ±4	±3 ±2			
$P11$ ** $P11$	1910 (theory) 1850–1990 (expt) 1955 (theory)	1.8 3 ±3 3.5	+7.1 +8 ±3 −4.0	+1.9 −3 ±2 +1.1	+2.5 +2.2		
$P11$ not seen	2025	2.4	−0.2	+1.3	−6.6		relatively inelastic
$P11$ not seen	2080	0.3	−1.1	+4.9	+0.1		decoupled from $\bar{K}N$
$P11$ not seen	2165	0.9	+0.4	−1.8	−0.7		decoupled from $\bar{K}N$

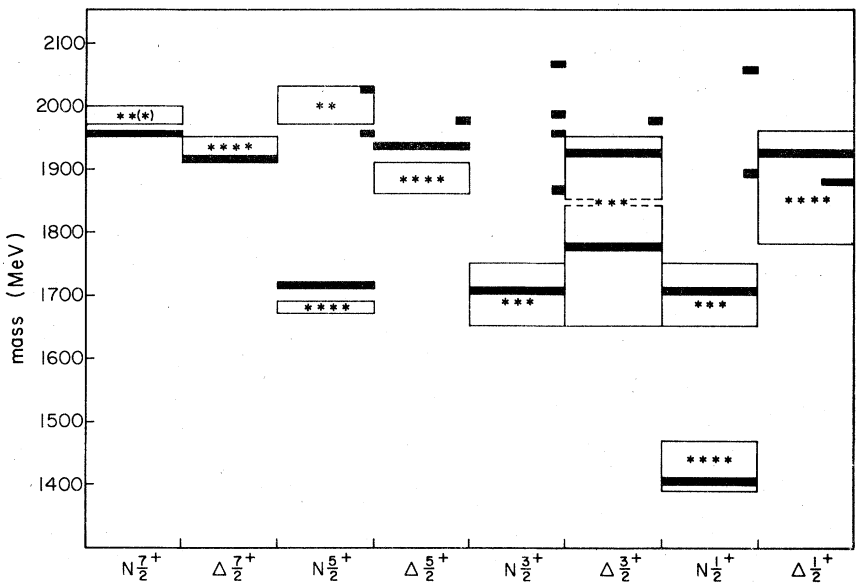

FIG. 3. The pattern of decouplings in the $S=0$ positive-parity excited baryons. The regions in which the masses of observed resonances probably lie are denoted by open boxes, in which are given the resonances' ratings according to Ref. 25. The predicted resonances are denoted by bars whose lengths indicate their predicted visibility relative to the strongest resonance in the partial wave. The legend is (1) full-length bar: greater than $\frac{1}{3}$ of the peak elastic amplitude of the strongest resonance; (2) $\frac{1}{3}$-length bar: $\frac{1}{6}$ to $\frac{1}{3}$ of the peak elastic amplitude of the strongest resonance; (3) stub: less than $\frac{1}{6}$ of the peak elastic amplitude of the strongest resonance. For these purposes we have used a very crude semiempirical formula for the total width of resonance R: $\Gamma_{\text{total}} \simeq \frac{1}{3}(M_R - M_0)\theta(M_R - M_0) + \Gamma_{\text{calc}}$, where Γ_{calc} is the width we calculate into quasi-two-body modes, $M_0 = 1550$ MeV, and $\theta(x) = 0$ or 1 as x is <0 or >0.

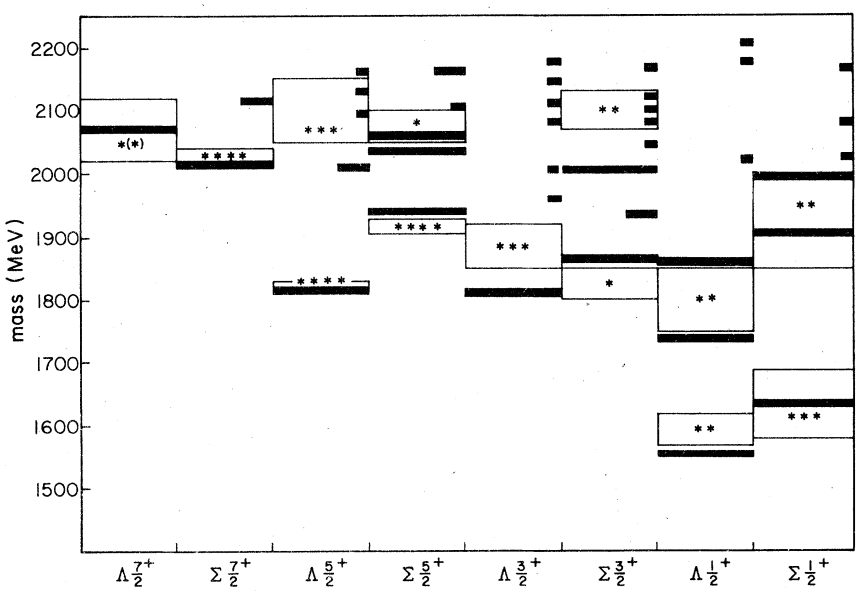

FIG. 4. The pattern of decouplings in the $S=-1$ positive-parity excited baryons. The coding here is as in Fig. 3 except that the elastic amplitude is taken to be the sum of the magnitudes of the peak amplitudes from $N\bar{K}$ to $N\bar{K}$, $\Sigma\pi$, and $\Lambda\pi$ and M_0 is taken to be 1700 MeV to allow for the higher $S=-1$ inelastic threshold.

with the correct couplings to both $N\pi$ and $\Delta\pi$.

(d) To complete this partial listing of hyperfine interaction mixing effects, we mention the hyperfine-induced admixture of non-^2S_S configurations into the ground-state octet.[24] This admixture provides explanations for the nonzero values of $\Lambda(1830)\frac{5}{2}^- \to N\bar{K}$, $N(1670)\frac{5}{2}^- \to p\gamma$ in $A^p_{1/2}$ and $A^p_{3/2}$, $\Lambda(2020)\frac{7}{2}^+ \to N\bar{K}$, $N(1990)\frac{7}{2}^+ \to p\gamma$ in $A^p_{1/2}$ and $A^p_{3/2}$, $N(1670)\frac{5}{2}^- \to \Lambda K$, and $N(1990)\frac{7}{2}^+ \to \Lambda K$.

The preceding praises of our model have been so ardent that we now feel obliged to point out that while it does adequately reproduce hundreds of amplitudes, there are a few probable discrepancies as well (see, e.g., the $P13$ photon amplitudes).

On this note we conclude our brief discussion of the tables. The model is clearly crude and of limited numerical accuracy; we nevertheless believe that the evidence is that it provides a good basis for an understanding of at least the salient features of baryon physics.

ACKNOWLEDGMENTS

Both of us would like to thank the Department of Theoretical Physics at Oxford for its generous hospitality during the period when this work was begun. In addition, we would like to acknowledge the collaboration of Gabriel Karl not only in the work upon which this paper was built, but also in the early stages of this project. Thanks also go to Stephen Godfrey. Finally, R.K. would like to acknowledge the importance of the continued encouragement of V. Koniuk. This research was supported in part by the Natural Sciences and Engineering Research Council of Canada.

APPENDIX

In order to maximize the usefulness of our compilations, we devote this appendix to making all of our conventions explicit by displaying our wave functions, Clebsch-Gordan conventions, partial-wave-helicity conversions, etc.

1. Flavor wave functions

ρ-type octet:

$$\phi^\rho_p = \frac{1}{\sqrt{2}}(udu - duu), \tag{A1}$$

$$\phi^\rho_{\Sigma^+} = \frac{1}{\sqrt{2}}(suu - usu), \tag{A2}$$

$$\phi^\rho_\Lambda = \frac{1}{\sqrt{12}}(2uds - 2dus + usd - dsu - sud + sdu), \tag{A3}$$

$$\phi^\rho_{\Xi^0} = \frac{1}{\sqrt{2}}(sus - uss). \tag{A4}$$

λ-type octet:

$$\phi^\lambda_p = \frac{-1}{\sqrt{6}}(udu + duu - 2uud), \tag{A5}$$

$$\phi^\lambda_{\Sigma^+} = \frac{1}{\sqrt{6}}(suu + usu - 2uus), \tag{A6}$$

$$\phi^\lambda_\Lambda = \frac{1}{2}(usd - dsu + sud - sdu), \tag{A7}$$

$$\phi^\lambda_{\Xi^0} = \frac{-1}{\sqrt{6}}(sus + uss - 2ssu). \tag{A8}$$

Decuplet:

$$\phi^S_{\Delta^{++}} = uuu, \tag{A9}$$

$$\phi^S_{\Sigma^+} + \frac{1}{\sqrt{3}}(uus + usu + suu), \tag{A10}$$

$$\phi^S_{\Xi^0} = \frac{1}{\sqrt{3}}(ssu + sus + uss), \tag{A11}$$

$$\phi^S_\Omega = sss. \tag{A12}$$

Singlet:

$$\phi^A_\Lambda = \frac{1}{\sqrt{6}}(uds - dus - usd + dsu + sud - sdu). \tag{A13}$$

All other wave functions follow from the Condon-Shortley convention. These wave functions have themselves been chosen to conform to the SU(3) conventions of de Swart,[25,31] and *differ from the wave functions used in Refs. 1–4 by various minus signs*. A dictionary for translating the results of these references into the present "standard" conventions is given in subsection 7 of this Appendix.

2. Spin wave functions

ρ-type spin $\frac{1}{2}$:

$$\chi^\rho_+ = \frac{1}{\sqrt{2}}(\uparrow\downarrow\uparrow - \downarrow\uparrow\uparrow). \tag{A14}$$

λ-type spin $\frac{1}{2}$:

$$\chi^\lambda_+ = \frac{-1}{\sqrt{6}}(\uparrow\downarrow\uparrow + \downarrow\uparrow\uparrow - 2\uparrow\uparrow\downarrow). \tag{A15}$$

Spin $\frac{3}{2}$:

$$\chi^s_{+3/2} = \uparrow\uparrow\uparrow. \tag{A16}$$

All others follow from the Condon-Shortley convention.

3. Spatial wave functions

With[32]

$$\vec{\rho} = \frac{1}{\sqrt{2}}(\vec{r}_1 - \vec{r}_2), \tag{A17}$$

$$\vec{\lambda} = \frac{1}{\sqrt{6}}(\vec{r}_1 + \vec{r}_2 - 2\vec{r}_3), \tag{A18}$$

we choose the three-body harmonic-oscillator wave functions in the SU(3) limit to be

$$\psi^{\sigma}_{lm} \equiv \Psi^{\sigma}_{lm} \frac{\alpha^3}{\pi^{3/2}} \exp[-\tfrac{1}{2}\alpha^2(\rho^2+\lambda^2)], \tag{A19}$$

where with $A_{\pm} \equiv A_x \pm iA_y$ we have

$$\Psi^S_{00} = 1, \tag{A20}$$

$$(\Psi^{\rho}_{11}, \Psi^{\lambda}_{11}) = \alpha(\rho_+, \lambda_+), \tag{A21}$$

$$\Psi^{S'}_{00} = \frac{1}{\sqrt{3}}\alpha^2(\rho^2+\lambda^2-3\alpha^{-2}), \tag{A22}$$

$$(\Psi^{\rho}_{00}, \psi^{\lambda}_{00}) = \frac{1}{\sqrt{3}}\alpha^2(2\vec{\rho}\cdot\vec{\lambda}, \rho^2-\lambda^2), \tag{A23}$$

$$\Psi^S_{22} = \tfrac{1}{2}\alpha^2(\rho_+^2+\lambda_+^2), \tag{A24}$$

$$(\Psi^{\rho}_{22}, \Psi^{\lambda}_{22}) = \tfrac{1}{2}\alpha^2(2\rho_+\lambda_+, \rho_+^2-\lambda_+^2), \tag{A25}$$

$$\Psi^A_{11} = \alpha^2(\rho_+\lambda_z - \rho_z\lambda_+). \tag{A26}$$

As usual, the remaining wave functions follow from the Condon-Shortley convention.

4. SU(6) × O(3) wave functions

We use interchangeably the two notations

$$|X^{2S+1}M[\mu, L^P]J^P\rangle \equiv |X_M{}^{2S+1}L_{\sigma}J^P\rangle,$$

where $X = p, n, \ldots$, M and μ are the SU(3) and SU(6) multiplicities, S, L, P, and J are the total quark spin, total orbital angular momentum, parity, and total angular momentum, and σ is the symmetry of μ (S = symmetric ⟷ 56, M = mixed ⟷ 70, and A = antisymmetric ⟷ 20). We prefer the latter notation since it is readily extended to the *uds* basis which is so useful when SU(3) is broken. For the states of highest $J = L + S$ we take

$$|X_8{}^2L_S(L+\tfrac{1}{2})^P\rangle = \frac{1}{\sqrt{2}}(\chi^{\rho}_+\phi^{\rho}_X + \chi^{\lambda}_+\phi^{\lambda}_X)\psi^S_{LL}, \tag{A27}$$

$$|X_8{}^2L_M(L+\tfrac{1}{2})^P\rangle = \frac{1}{2}(\chi^{\rho}_+\phi^{\rho}_X\psi^{\lambda}_{LL} + \chi^{\rho}_+\phi^{\lambda}_X\psi^{\rho}_{LL} + \chi^{\lambda}_+\phi^{\rho}_X\psi^{\rho}_{LL} - \chi^{\lambda}_+\phi^{\lambda}_X\psi^{\lambda}_{LL}), \tag{A28}$$

$$|X_8{}^2L_A(L+\tfrac{1}{2})^P\rangle = \frac{1}{\sqrt{2}}(\chi^{\rho}_+\phi^{\lambda}_X - \chi^{\lambda}_+\phi^{\rho}_X)\psi^A_{LL}, \tag{A29}$$

$$|X_8{}^4L_M(L+\tfrac{3}{2})^P\rangle = \frac{1}{\sqrt{2}}(\phi^{\rho}_X\psi^{\rho}_{LL} + \phi^{\lambda}_X\psi^{\lambda}_{LL})\chi^S_{+3/2}, \tag{A30}$$

$$|X_{10}{}^2L_M(L+\tfrac{1}{2})^P\rangle = \frac{1}{\sqrt{2}}(\chi^{\rho}_+\psi^{\rho}_{LL} + \chi^{\lambda}_+\psi^{\lambda}_{LL})\phi^S_X, \tag{A31}$$

$$|X_{10}{}^4L_S(L+\tfrac{3}{2})^P\rangle = \chi^S_{+3/2}\phi^S_X\psi^S_{LL}, \tag{A32}$$

$$|\Lambda_1{}^2L_M(L+\tfrac{1}{2})^P\rangle = \frac{1}{\sqrt{2}}(\chi^{\rho}_+\psi^{\lambda}_{LL} - \chi^{\lambda}_+\psi^{\rho}_{LL})\phi^A_{\Lambda}, \tag{A33}$$

$$|\Lambda_1{}^4L_A(L+\tfrac{3}{2})^P\rangle = \chi^3_{+3/2}\phi^A_{\Lambda}\psi^A_{LL}. \tag{A34}$$

States with $J < L + S$ are constructed by using standard tables[25] in the LS order with the above states as a guide for overall minus signs; states with smaller J_z follow from the Condon-Shortley convention.

5. Photon-amplitude conventions

We follow the conventions of the Particle Data Group[25] and others by quoting in Table VII the values of the photon amplitudes obtained via Table III times the sign of the $A_{1/2}N\pi$ amplitude (see subsection 6 below) with an additional factor of -1 $(+1)$ for the photoproduction of an N^* (Δ^*) resonance.

6. Conversion from the helicity to the partial-wave basis

The text provides a description of how to calculate helicity amplitudes. We use these essentially directly for photons (see subsection 5 of this Appendix), but for pseudoscalar emission we always convert to the more common partial-wave basis. Table XII provides the conversion factors. In addition to this conversion the amplitudes quoted in the tables have been multiplied by $(2J_R+1)^{-1/2}$ so that their squares are actually the channel partial widths. [See Eq. (8) and note that the kinematic factors have been included in our definitions of the partial-wave amplitudes of Tables I and V.]

7. A translation dictionary for baryon compositions

There are many sign conventions in the literature; in this paper we have attempted to establish a convenient and explicit set of conventions both for the baryons and the emitted mesons (for example, the X^M of Sec. III also satisfy the de Swart conventions). Since the authors of Refs. 1–4 arranged their conventions to facilitate comparison with previous decay analyses, they are not always identical to the ones used here. Since the baryon compositions and the decay amplitudes must be in the same conventions before they are folded together, we provide here a set of rules for converting these published baryon compositions to the standard conventions of this paper:

(1) In the $(70, 1^-)$ the mixing coefficients of $N^2P_{M\frac{3}{2}^-}$, $N^2P_{M\frac{1}{2}^-}$, $\Lambda_8{}^4P_{M\frac{3}{2}^-}$, $\Lambda_8{}^4P_{M\frac{1}{2}^-}$, $\Sigma_8{}^2P_{M\frac{3}{2}^-}$, and $\Sigma_8{}^2P_{M\frac{1}{2}^-}$ in Ref. 3 must have their signs changed [for the Ξ's see (3) below].

(2) In the positive-parity excited states all Λ_8 and Σ_8 mixing coefficients in Ref. 4 must have

TABLE XII. Conversion from helicity to partial-wave amplitudes.

J_{initial}	P_{initial}	$J^P_{\text{final}}=\frac{1}{2}^+$	$J^P_{\text{final}}=\frac{3}{2}^+$	
$\frac{1}{2}$	−	$A_{1/2}=+A_S$	$A_{1/2}=+A_D$	
	+	$A_{1/2}=-A_P$	$A_{1/2}=-A_P$	
$\frac{3}{2}$	+	$A_{1/2}=+A_P$	$A_{3/2}=-(\frac{9}{10})^{1/2}A_P-(\frac{1}{10})^{1/2}A_F$,	$A_{1/2}=-(\frac{1}{10})^{1/2}A_P+(\frac{9}{10})^{1/2}A_F$
	−	$A_{1/2}=-A_D$	$A_{3/2}=+(\frac{1}{2})^{1/2}A_S+(\frac{1}{2})^{1/2}A_D$,	$A_{1/2}=+(\frac{1}{2})^{1/2}A_S-(\frac{1}{2})^{1/2}A_D$
$\frac{5}{2}$	−	$A_{1/2}=+A_D$	$A_{3/2}=-(\frac{6}{7})^{1/2}A_D-(\frac{1}{7})^{1/2}A_G$,	$A_{1/2}=-(\frac{1}{7})^{1/2}A_D+(\frac{6}{7})^{1/2}A_G$
	+	$A_{1/2}=-A_F$	$A_{3/2}=+(\frac{2}{5})^{1/2}A_P+(\frac{3}{5})^{1/2}A_F$,	$A_{1/2}=+(\frac{3}{5})^{1/2}A_P-(\frac{2}{5})^{1/2}A_F$
$\frac{7}{2}$	+	$A_{1/2}=+A_F$	$A_{3/2}=-(\frac{5}{6})^{1/2}A_F-(\frac{1}{6})^{1/2}A_H$,	$A_{1/2}=-(\frac{1}{6})^{1/2}A_F+(\frac{5}{6})^{1/2}A_H$
	−	$A_{1/2}=-A_G$	$A_{3/2}=+(\frac{5}{14})^{1/2}A_D+(\frac{9}{14})^{1/2}A_G$,	$A_{1/2}=+(\frac{9}{14})^{1/2}A_D-(\frac{5}{14})^{1/2}A_G$

their signs changes. Note that there are two errors in Table VI of Ref. 4: ${}^4\Sigma_{10}D_M\frac{7}{2}^+$ should read ${}^4\Sigma_8D_M\frac{7}{2}^+$, and ${}^2\Lambda_1D_M\frac{5}{2}^+$ should be interchanged with ${}^2\Lambda_8D_M\frac{5}{2}^+$.

(3) All other coefficients are unchanged provided that all Ξ compositions are taken from the more recent Ref. 7 and not from Ref. 3.

8. Composition of the ground-state baryons with $J^P=\frac{1}{2}^+$

The calculation of SU(6)-violating amplitudes which proceed via the admixture of non-^2S_S components in the ground states requires knowledge of the mixing coefficients of the various impurities, and especially of the ^2S_M components. With the exception of the nucleon, these have not been given previously; by the methods discussed in Ref. 24 one obtains

$$N(940)\simeq 0.90N\,{}^2S_S-0.34N\,{}^2S'_S-0.27N\,{}^2S_M-0.06N\,{}^4D_M, \tag{A35}$$

$$\Lambda(1115)\simeq 0.93\Lambda_8\,{}^2S_S-0.30\Lambda_8\,{}^2S'_S-0.20\Lambda_8\,{}^2S_M-0.05\Lambda_1\,{}^2S_M-0.03\Lambda_8\,{}^4D_M, \tag{A36}$$

$$\Sigma(1195)\simeq 0.97\Sigma_8\,{}^2S_S-0.18\Sigma_8\,{}^2S'_S-0.16\Sigma_8\,{}^2S_M-0.02\Sigma_{10}\,{}^2S_M-0.05\Sigma_8\,{}^4D_M+0.02\Sigma_{10}\,{}^4D_M, \tag{A37}$$

$$\Xi(1320)\simeq 0.95\Xi_8\,{}^2S_S-0.25\Xi_8\,{}^2S'_S-0.16\Xi_8\,{}^2S_M-0.01\Xi_{10}\,{}^2S_M-0.03\Xi_8\,{}^4D_M-0.01\Xi_{10}\,{}^4D_M. \tag{A38}$$

[1]Nathan Isgur and Gabriel Karl, Phys. Lett. 72B, 109 (1977).

[2]Nathan Isgur and Gabriel Karl, Phys. Lett. 74B, 353 (1978).

[3]Nathan Isgur and Gabriel Karl, Phys. Rev. D 18, 4187 (1978).

[4]Nathan Isgur and Gabriel Karl, Phys. Rev D 19, 2653 (1979); erratum (to be published).

[5]L. A. Copley, Nathan Isgur, and Gabriel Karl, Phys. Rev. D 20, 768 (1979).

[6]Nathan Isgur and Gabriel Karl, Phys. Rev. D 20, 1191 (1979).

[7]K.-T. Chao, Nathan Isgur, and Gabriel Karl, University of Toronto report, 1980 (unpublished).

[8]Nathan Isgur, Lectures at the XVI International School of Subnuclear Physics, Erice, Italy, 1978 (unpublished).

[9]Gabriel Karl, in *Proceedings of the 19th International Conference on High Energy Physics, Tokyo, 1978*, edited by S. Homma, M. Kawaguchi, and H. Miyazawa (Phys. Soc. of Japan, Tokyo, 1979), p. 135.

[10]O. W. Greenberg, Annu. Rev. Nucl. Part. Sci. 28, 327 (1978).

[11]A. J. G. Hey, Southampton report, 1978 (unpublished); summary talk presented at the 1979 EPS International Conference on High Energy Physics, Southampton report (unpublished).

[12]O. W. Greenberg, Phys. Rev. Lett. 13, 598 (1964); O. W. Greenberg and M. Resnikoff, Phys. Rev. 163, 1844 (1967); D. R. Digvi and O. W. Greenberg, *ibid.* 175, 2024 (1968); H. Resnikoff, Phys. Rev. D 3, 199 (1971).

[13]R. H. Dalitz, in *High Energy Physics, Ecole d'Eté de Physique Théorique, Les Houches, 1963*, edited by C. Dewitt and M. Jacob (Gordon and Breach, New York, 1966); R. R. Horgan and R. H. Dalitz, Nucl. Phys. B66, 135 (1973); R. R. Horgan, *ibid.* B71, 514 (1974); M. Jones, R. R. Horgan, and R. H. Dalitz, *ibid.* B129, 45 (1977); R. H. Dalitz and L. J. Reinders, in Proceedings of the Hadron Structure'77 Conference, Slovak Academy of Sciences, Bratislava, 1978 (unpub-

lished).
[14]A. De Rújula, H. Georgi, and S. L. Glashow, Phys. Rev. D 12, 147 (1975); T. DeGrand, R. L. Jaffe, K. Johnson, and J. Kiskis, *ibid.* 12, 2060 (1975).
[15]For work on baryons related to the model of Refs. 1–11 see D. Gromes and I. O. Stamatescu, Nucl. Phys. B112, 213 (1976); W. Celmaster, Phys. Rev. D 15, 139 (1977); D. Gromes, Nucl. Phys. B130, 18 (1977); B131, 80 (1977); U. Ellwanger, *ibid.* B139, 422 (1978); L. J. Reinders, J. Phys. G 4, 1241 (1978); A. Le Yaouanc *et al.*, Phys. Rev. D 18, 1591 (1978); I. M. Barbour and D. K. Ponting, Glasgow University reports, 1979 (unpublished); M. Bohm, Wurzburg University report, 1979; Paul Fage, Oxford University doctoral thesis, 1979 (unpublished).
[16]For work on mesons related to the model of Refs. 1–11 see H. J. Schnitzer, Phys. Lett. 65B, 239 (1976); 69B, 477 (1977); Phys. Rev. D 18, 3482 (1978); R. H. Graham and P. J. O'Donnell, *ibid.* 19, 284 (1979); B. R. Martin and L. J. Reinders, Nucl. Phys. B143, 309 (1978); Phys. Lett. 78B, 144 (1978); A. B. Henriques, B. Kellet, and R. G. Moorhouse, Phys. Lett. 64B, 85 (1976); L. Him Chan, Phys. Lett. 71B, 422 (1977); R. Barbieri *et al.*, Nucl. Phys. B105, 125 (1976); E. Eichten *et al.*, Phys. Rev. D 17, 3090 (1978); M. Krammer and M. Krasemann, DESY Report No. 79/20, 1979 (unpublished); L. J. Reinders, University College London report, 1979 (unpublished); I. Cohen and H. J. Lipkin, Nucl. Phys. B112, 213 (1976); J. Arafune, M. Fukugita, and Y. Oyanagi, Phys. Rev. D 16, 772 (1977); A. Bradley and F. D. Gault, Durham/Manchester report, 1978 (unpublished); A. Bradley and D. Robson, Manchester report 1979, (unpublished); A. Bradley, Manchester report, 1979 (unpublished).
[17]This model is very similar to some preconfinement models. See H. J. Lipkin, Phys. Lett. 45B, 267 (1973); Y. Nambu, in *Preludes in Theoretical Physics*, edited by A. de Shalit, H. Feshbach, and L. van Hove (North-Holland, Amsterdam, 1966).
[18]C. Becchi and G. Morpurgo, Phys. Rev. 149, 1284 (1966); 140B, 687 (1965); Phys. Lett. 17, 352 (1965); A. N. Mitra and M. Ross, Phys. Rev. 158, 1630 (1967); D. Faiman and A. W. Hendry, *ibid.* 173, 1720 (1968); H. J. Lipkin, Phys. Rep. 8C, 173 (1973); J. L. Rosner, *ibid.* 11C, 189 (1974); R. Horgan, in *Proceedings of the Topical Conference on Baryon Resonances, Oxford, 1976*, edited by R. T. Ross and D. H. Saxon (Rutherford Laboratory, Chilton, Didcot, England, 1976); A. Le Yaouanc *et al.*, Phys. Rev. D 11, 1272 (1975).
[19]L. A. Copley, G. Karl, and E. Obryk, Phys. Lett. 29B, 117 (1969); L. A. Copley, G. Karl, and E. Obryk, Nucl. Phys. B13, 303 (1969); D. Faiman and A. W. Hendry, Phys. Rev. 180, 1572 (1969); Kohichi Ohta, Phys. Rev. Lett. 43, 1201 (1979). The Copley, Karl, and Obryk value of $\alpha = 0.41$ GeV which we have adopted for our decay analysis differs somewhat from the value of 0.32 GeV found in the spectroscopic applications (see Ref. 6) of the harmonic-oscillator model.
[20]R. G. Moorhouse, Phys. Rev. Lett. 16, 771 (1966).
[21]H. Lipkin and S. Meshkov, Phys. Rev. Lett. 14, 670 (1965); D. Faiman and A. W. Hendry, Phys. Rev. 173, 1720 (1968); 180, 1609 (1969); E. W. Colglazier and J. L. Rosner, Nucl. Phys. B27, 349 (1971); W. Petersen and J. Rosner, Phys. Rev. D 6, 820 (1972); A. J. G. Hey, P. J. Litchfield, and R. J. Cashmore, Nucl. Phys. B95, 516 (1975); F. Gilman and I. Karliner, Phys. Rev. D 10, 2194 (1974); J. Babcock and J. Rosner, Ann. Phys. (N.Y.) 96, 191 (1976); J. Babcock *et al.*, Nucl. Phys. B126, 87 (1977).
[22]R. P. Feynman, M. Kislinger, and F. Ravndal, Phys. Rev. D 3, 2706 (1971); R. G. Moorhouse and N. H. Parsons, Nucl. Phys. B62, 109 (1973).
[23]Nathan Isgur, Phys. Rev. D 13, 122 (1976).
[24]Nathan Isgur, Gabriel Karl, and Roman Koniuk, Phys. Rev. Lett. 41, 1269 (1978).
[25]Particle Data Group, Phys. Lett. 75B, 1 (1978).
[26]Most of the experimental data are contained in Ref. 25 but our quotations have been influenced by recent analyses. In photoproduction: I. M. Barbour, R. L. Crawford and N. H. Parsons, Nucl. Phys. B141, 253 (1978); M. Fukushima *et al.*, *ibid.* B130, 486 (1977). In strong decays: W. A. Morris *et al.*, Phys. Rev. D 17, 55 (1978); D. E. Novoseller, Nucl. Phys. B137, 509 (1978); R. D. Baker *et al.*, Nucl. Phys. B156, 93 (1979); R. E. Cutkosky *et al.*, Carnegie-Mellon/Lawrence Berkeley Lab. report, 1979 (unpublished); D. M. Chew, Lawrence Berkeley Lab. report, 1979 (unpublished).
[27]P. J. Litchfield *et al.*, Nucl. Phys. B74, 39 (1974).
[28]This pattern of decouplings had been noticed empirically; see W. P. Petersen and J. L. Rosner, Phys. Rev. D 6, 820 (1972); D. Faiman, *ibid.* 15, 854 (1977).
[29]D. B. Lichtenberg, Phys. Rev. 178, 2197 (1968); S. Ono, Prog. Theor. Phys. 48, 964 (1972); R. H. Capps, Phys. Rev. Lett. 33, 1637 (1974); Phys. Rev. D 12, 3606 (1975); A. N. Mitra, Ann. Phys. (N.Y.) 43, 126 (1967); Nucl. Phys. B5, 308 (1968); Nuovo Cimento 56, 1164 (1968); J. F. Gunion and R. S. Willey, Phys. Rev. D 12, 174 (1975). See also Hey, Litchfield, and Cashmore in Ref. 21.
[30]That the properties of the $\Delta\frac{5}{2}^+$ resonance could be understood in terms of $(56, 2^+)$-$(70, 2^+)$ mixing was proposed by D. Faiman, J. L. Rosner, and J. Weyers, Nucl. Phys. B57, 45 (1973). Quark hyperfine interactions provide a dynamical mechanism that supplies the sign and magnitude of mixing that was suggested by these authors on empirical grounds.
[31]J. J. de Swart, Rev. Mod. Phys. 35, 916 (1963).
[32]G. Karl and E. Obryk, Nucl. Phys. B8, 609 (1968).